ment of dichloromethane (CH_2Cl_2) performed by Atlas *et al.* (National Center for Atmospheric Research), and a measurement of CO by Sachse *et al.* (NASA Langley Research Center) (*11*). The CO data were averaged over 1-min intervals to approximate the spatial range of the other measurements; the variability was calculated directly from this set (Table 2). Based on the curve generated by our data and the empirical variabilities of these three gases, the predicted values for τ are in reasonable agreement with the accepted values for these compounds. This corroboration adds confidence to our predicted value for τ_{CH_3Br}, because the other data sets were collected by independent research groups over sampling intervals and spatial ranges incongruent with our set.

Considering the more complete latitudinal coverage in the Southern Hemisphere and the more remote location of those samples, we believe the Southern Hemispheric prediction more closely simulates the assumptions necessary for application of the Junge relation to spatial variability estimates. The question of whether the variability has a seasonal signal could not be addressed by this data set but may be accessible in the future. A more complete latitudinal profile including the Northern Hemisphere might improve this analysis. Nonetheless, it seems unlikely that the residence time of CH_3Br lies outside the range 0.7 to 0.9 years.

References and Notes

1. *Scientific Assessment of Ozone Depletion: 1994, Les Diablerets, Switzerland, 19 to 21 July 1994* (University of Colorado at Boulder Publications Service, Colorado, 1995).
2. R. J. Cicerone and W. K. Ko, paper presented at the *1997 Methyl Bromide State of the Science Workshop*, Monterey, CA, 10 to 12 June 1997. Sponsored by the Methyl Bromide Global Coalition in cooperation with NASA.
3. S. A. Yvon-Lewis and J. H. Butler, *Geophys. Res. Lett.* **24**, 1227 (1997).
4. C. E. Junge, *Air Chemistry and Radioactivity* (Academic Press, New York, London, 1963).
5. A. G. Gibbs and W. G. N. Slinn, *J. Geophys. Res.* **78**, 574 (1973).
6. M. B. Baker, H. Harison, J. Vinelli, K. B. Erickson, *Tellus* **31**, 39 (1979).
7. R. Jaeschke, in *Chemistry of the Unpolluted and Polluted Troposphere*, H. W. Georgii and W. Jaeschke, Eds. (Reidel, Boston, 1982), pp. 341–373.
8. W. G. N. Slinn, *Tellus* **40B**, 229 (1988).
9. C. E. Junge, *ibid.* **26**, 477 (1974).
10. M. Hamrud, *ibid.* **35B**, 295 (1983).
11. Details about the PEM missions can be found in http://www-gte.larc.nasa.gov/pem/pemt_hmpg.htm and links therein. The data set used in this analysis can be found in files contained within ftp://ftp-gte.larc.nasa.gov/pub/PEMTROPICSA.
12. R. G. Prinn *et al.*, *Science* **269**, 187 (1995).
13. M. Prather and C. M. Spivakovsky, *J. Geophys. Res.* **95**, 18723 (1990).
14. W. B. DeMore *et al.*, *Chemical Kinetics and Photochemical Data for use in Stratospheric Modeling* (Publication 97-4, Jet Propulsion Laboratory, California Institute of Technology, Pasadena, CA, 1997), vol. 12.
15. C. J.-L. Wang, D. R. Blake, F. S. Rowland, *Geophys. Res. Lett.* **22**, 1097 (1995).
16. J. H. Shorter *et al.*, *Nature* **337**, 717 (1995); D. B. King and E. S. Saltzman, *J. Geophys. Res.* **102**, 18715 (1997); S. Elliott and F. S. Rowland, *Geophys. Res. Lett.* **20**, 1043 (1993).
17. In this context, a recently discoveryed biological sink for CH_3Br in the polar oceans is not thought to be present for the other four compounds. The distribution and seasonality of this sink is still highly uncertain, and some portions of the ocean may also be a source of CH_3Br. Regardless, no evidence for a large sink in the southern boundary layer was seen in this data set (Fig. 3B, and discussion in paragraph 6). If a large oceanic sink were affecting the variability of CH_3Br in a nonspatially uniform manner, it would be expected to increase its empirical variability relative to the other four compounds. Therefore, any correction due to this effect would have to subtract from its stated variability and thus increase our residence time prediction.

18. We acknowledge the hard work and commitment to excellence exhibited by the science team at the University of California at Irvine and all members of the PEM Tropics mission. Funding was provided by NASA grant NAG-1-1777.

16 March 1998; accepted 27 May 1998

Water as a Dense Icelike Component in Silicate Glasses

P. Richet and A. Polian

Density and Brillouin-scattering measurements of hydrous andesite glasses at ambient conditions showed that dissolved water has a concentration-independent partial molar volume of 12 ± 0.5 cubic centimeters per mole and a bulk modulus of 18 ± 3 gigapascals. Dissolved as hydroxyl ions or as molecular water, water has volume properties similar to those of ice VII, the densest form of ice. These properties point to hydrogen bonding as an important factor in water dissolution, and they indicate that changes of water speciation are driven by the entropy and not by the volume of the system. Water in a concentration greater than 1 percent by weight also causes a marked decrease of the shear modulus of the glass.

Water is an important component of naturally occurring silicate glasses and melts. As a light oxide, it influences the density of the melt, which affects the rate of magma ascent. The effects of water on volume properties are generally not well known, however. For glasses, reported partial molar volumes of water range from 0 to 22 cm^3/mol at room pressure (*1*), and elastic properties have not been investigated. Here, we show that, in conjunction with density measurements, Brillouin scattering can be used to determine the elastic moduli of hydrous glasses. Because the elastic moduli are related to the bonding within a substance, these measurements provide structural information on water dissolution and speciation.

Because of the importance of water in andesitic lavas, we investigated a glass whose composition was similar to that of andesitic Montagne Pelée lavas that formed 650 years before the present in the last pumice eruption (*2*). Glasses made from the lavas (ME1311 in Table 1) would have been opaque, so we investigated hydrous iron-free glasses that had been used in viscosity measurements (*3*). After synthesis from oxide and carbonate mixtures, the starting glass (Table 1) was hydrated with up to 3.5 weight % H_2O at high pressure and high temperature in an internally heated vessel. The anhydrous natural and synthetic materials had the same viscosity, and analyses of the water content indicated that water dissolution was homogeneous in the synthetic glasses (*3*).

The Brillouin-scattering measurements (Table 2) were made with a setup similar to that previously described (*4*), whereby the light scattered by the sample from the single-mode 200-mW beam of an Ar^+ laser tuned to 514.5 nm was analyzed by a six-pass tandem Fabry-Pérot interferometer and was recorded with a photon-counting multichannel detector. The longitudinal (V_p) and shear (V_s) sound velocities were determined to within 30 m/s from spectra recorded in about 5 min with a platelet geometry. These results were then used to determine (to within 1%) the index of refraction (n) from experiments that were performed with a backscattering geometry. The investigated samples were doubly polished thin sections that were previously used to record infrared (IR) spectra before and after viscosity measurements (*3*).

A first series of measurements was made on samples that were recovered after hydration at high pressure, which were thus densified permanently (*5*). A second series was made on samples whose densities had relaxed to the room-pressure values while being heated during the viscosity measurements (*3*); as shown from Archimedean measurements of the density (ρ), the latter samples were less

---

P. Richet, Laboratoire de Physique des Géomatériaux, Unité de Recherche Associée CNRS 734, Institut de Physique du Globe, 4, Place Jussieu, 75252 Paris Cedex 05, France. A. Polian, Laboratoire de Physique des Milieux Condensés, Unité de Recherche Associée CNRS 782, Université Paris VI, 4, Place Jussieu, 75252 Paris Cedex 05, France.

Table 1. Glass compositions of Montagne Peleé lavas. ME1311e was measured by x-ray fluorescence analysis, and andesite was measured by an electron microprobe analysis (*3*). LOI, loss on ignition. Dash represents unavailable data.

Glass	ME1311e (weight %)	Andesite (weight %)
SiO_2	59.20	62.40 ± 0.69
Al_2O_3	18.10	20.01 ± 0.11
MgO	2.57	3.22 ± 0.05
CaO	7.15	9.08 ± 0.14
Na_2O	3.41	3.52 ± 0.07
K_2O	0.89	0.93 ± 0.05
TiO_2	0.52	0.55 ± 0.06
Fe_2O_3	7.52	0.03 ± 0.03
MnO	0.20	0.02 ± 0.03
P_2O_5	0.17	0.12 ± 0.03
LOI	0.85	–
Total	100.58	99.93

Table 2. Water content w_{H_2O}; density, ρ; Brillouin velocities, V_p and V_s; bulk modulus, K_S; compressibility, β_S; shear modulus, *G*; index of refraction, *n*; and fictive temperature T_f of the glasses (as given by the temperature at which the viscosity is 10^{12} Pa · s).

w_{H_2O} (weight %)	ρ (g/cm³)	V_p (km/s)	V_s (km/s)	K_S (GPa)	$10^{11}\beta_S$ (Pa^{-1})	*G* (GPa)	*n*	T_f (K)
				Compacted samples				
1.0	2.505	6.23	3.70	51.5	1.94	34.3	1.533	-
2.7	2.487	6.12	3.59	50.4	1.98	32.1	1.558	-
3.5	2.459	5.99	3.49	48.2	2.07	30.0	1.570	-
				Relaxed samples				
0	2.513	6.24	3.70	52.0	1.92	34.4	1.541	1017
0.3	2.507	6.25	3.73	51.4	1.94	34.9	1.538	955
1.0	2.497	6.23	3.75	50.1	2.00	35.1	1.535	870
2.7	2.465	6.06	3.55	49.1	2.04	31.1	1.564	757
3.5	2.437	6.09	3.62	47.8	2.09	31.9	1.551	735

dense than the former (Fig. 1). For the compacted samples, the partial molar volumes of water and the anhydrous glass are 11.46 (±0.28) and 25.52 (3 ± 0.03) cm³/mol, respectively. Both of these volumes are slightly higher for the relaxed samples, but the volume of water remains consistent with the value of 12 ± 0.5 cm³/mol found over the investigated compositional range of silicate glasses (*6*).

Similar to the full widths at half maximum of the Brillouin peaks (not included in Table 2), the index of refraction is practically independent of the water content. The sound velocities V_p and V_s remain practically constant up to 4 mole percent (mol%) H_2O before slightly decreasing at higher contents (Fig. 2). One would expect slightly higher velocities for the compacted samples, but the velocity differences are within the experimental error of the measurements. For the water-free glass, the shear modulus as given by $G = \rho V_s^2 = 34.4 \pm 0.7$ GPa is similar to the 32 GPa previously reported for a somewhat denser (ρ = 2.57 g/cm³) andesite glass of unspecified composition (*7*). Having the same compositional dependence as the shear velocity, *G* is initially constant at 35 ± 1 GPa before decreasing to about 31 GPa at 3.5 weight % H_2O. This decrease is so strong that extrapolation of this trend would result in a *G* value of 0 GPa before 100 mol% H_2O was reached.

As determined from $K_S = \rho\,(V_p^2 - 4/3\ V_S^2)$, the bulk modulus ($K_S$) decreases smoothly from 52.0 ± 1.4 GPa for the water-free glass, which is consistent with the previously reported modulus of 52.5 ± 0.8 GPa, to 48 GPa for samples with 12 mol% H_2O. Because of the small difference between the isobaric and isochoric heat capacities of silicate glasses (*8*), the same slight differences between the isothermal and adibatic bulk moduli can be neglected. The relaxed samples are more compressible than their compacted counterparts.

Water may dissolve in silicate glasses as hydroxyl ions (OH^-) and molecular water. For initial water contents less than about 3 weight %, the water predominately dissolves as OH^-. For water contents of 3 to 4 weight %, the water dissolves as about equal amounts of OH^- and H_2O. Above 4 weight %, water mainly dissolves as H_2O (*9, 10*). As determined from IR spectroscopy, water speciation in the present andesite samples conforms to these trends (*3*). Because the concentration of molecular water becomes significant above 1 weight % H_2O, it is tempting to relate the decrease in *G* observed beyond this content with the rapidly increasing concentration of molecular water.

Changing speciation has little effect on the volume and K_S of the water component, which indicates that the volume change of the reaction $O_b^{2-} + H_2O = 2OH^-$ (where O_b is a bridging oxygen of the silicate framework) is small at room pressure and remains small at pressure. This small volume change rules out any frequency dependence of the elastic moduli caused by possibly sluggish speciation reactions and also agrees with the fact that, at constant water content, few differences in water speciation are apparent from the IR spectra of our compacted and relaxed andesite glasses. Other support for small volume changes comes from the same speciation that was observed for two series of calcium aluminosilicate glasses that were prepared at 0.1 and 1.5 to 2.0 GPa and had densities differing by about 8% (*10*). Contrasting with this weak pressure dependence, the proportion of OH^- has been reported to increase with increasing temperature at the expense of H_2O (*11*). At least up to the glass transition, the changes in water speciation appear to be essentially driven by the entropy.

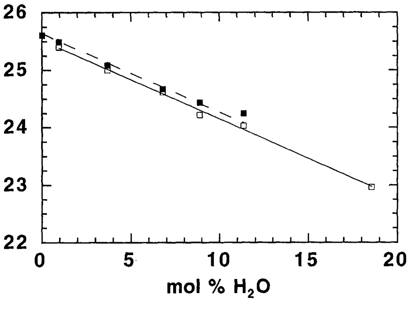

Fig. 1. Molar volume (*V*) of compacted (open squares) and relaxed (solid squares) hydrous andesite glasses. The water molar fractions have been calculated for the pseudobinary H_2O-andesite glass system on the basis of molar masses of 18.015 and 64.345 g for water and for the silicate end-member, respectively. For the silicate end-member, this basis corresponds to the usual total of 1 mol of oxide components. All of these samples were not available for the prevent Brillouin-scattering study.

Within the framework of the Adam-Gibbs configurational entropy theory of relaxation processes (*12*), the viscosity of silicate melts can be modeled quantitatively (*13*). As a temperature-induced process, water speciation should be relevant for the viscosity of hydrous melts. Mixing of OH^- and H_2O would, in effect, enhance the non-Arrhenian temperature dependence of the viscosity, which is determined by increases in configurational entropy. In addition, the 1-bar viscosity of andesite melts as measured above the glass transition joins smoothly with viscosities determined above the liquidus at high pressure (*3*). Because the vis-

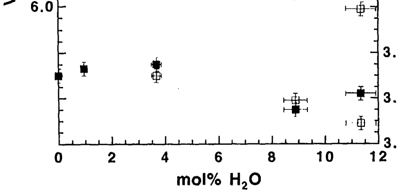

Fig. 2. V_p and V_S of compacted (open squares) and relaxed (solid squares) hydrous andesite glasses. Error bars in Figs. 2 through 4 indicate errors from water analyses and sound velocities.

cosity at constant temperature should depend to some extent on the relative abundances of OH^- and H_2O, this observation is consistent with a lack of pressure effects on water speciation up to superliquidus temperatures.

As determined from Fig. 3, the partial molar K_S of dissolved water is 18 ± 3 GPa, which is lower than the K_S values of geologically relevant silicate glasses, which range from 30 to 80 GPa (*7*). From obsidian to andesite and basalt compositions, for instance, K_S increases from 38 to 52 and 63 GPa, respectively, a trend that also correlates with the progressive disruption of the open network that is characteristic of silica-rich compositions. If our results for an andesite composition are representative of silicate glasses, the decreasing polymerization of the host silicate phase by water will enhance compressibility.

The partial molar volume of water in glasses (12 ± 0.5 cm^3/mol) is similar to 12.3 ± 0.3 cm^3/mol, which is the ambient volume of ice VII (*14*), the densest polymorph of ice near room temperature. We might expect structural differences between water dissolved in silicate glasses, as either OH^- or H_2O, and ice VII, which is made up of a three-dimensional open network of H_4O tetrahedra with a body-centered cubic oxygen sublattice. The K_S of dissolved water is also close to that of ice VII, namely, 23.9 ± 0.9 GPa (*14*). This high compressibility of ice VII stems from a shortening of the weaker hydrogen bonds. Even though the existence of OH^- and H_2O in glasses is well established, relatively little is known about their bonding to the host silicate phase. The fact that the compressibility of dissolved water is high and is independent of concentration suggests that a shortening of hydrogen bonds should also be a major compression mechanism for OH^- and H_2O. This shortening would also account for the decrease in shear modulus with water concentration (Fig. 4) and would point to a clustering of OH^-.

Similarities between the effects of water and alkali oxides have been revealed by viscosity (*15*) or electrical conductivity measurements (*16*). Water in glasses has a molar volume between those of Li_2O (9.3 cm^3/mol) and Na_2O (18.3 cm^3/mol) (*17*), but it is a component about two or three times more compressible than these alkali oxides (*18*). This property is additional evidence for compressible bonds between OH^- and H_2O and the silicate network, which are nonexistent for alkali oxides; it also agrees with the similarity in hydrogen bonding characteristics between OH^- and H_2O species in silicate glasses as revealed by NMR spectroscopy (*19*).

References and Notes

1. R. A. Lange, *Rev. Mineral.* **30**, 331 (1994).
2. B. Villemant, G. Boudon, J. C. Komorowski, *Earth Planet. Sci. Lett.* **140**, 259 (1996).
3. P. Richet *et al.*, *Chem. Geol.* **128**, 195 (1996).
4. J. R. Sandercock, in *Light Scattering in Solids III*, M. Cardona and G. Güntherodt, Eds. (Springer-Verlag, Berlin, 1982), pp. 173–206.
5. G. Tammann and E. Jenckel, *Z. Anorg. Allg. Chem.* **184**, 416 (1929).
6. P. Richet *et al.*, *Eos (Fall Suppl.)* **77**, 799 (1996).
7. J. D. Bass, in *Handbook of Physical Constants*, T. J. Ahrens, Ed. (American Geophysical Union, Washington, DC, 1995), vol. 2, pp. 45–63.
8. P. Richet and Y. Bottinga, *Geochim. Cosmochim. Acta* **44**, 1535 (1980).
9. E. Stolper, *Contrib. Mineral. Petrol.* **81**, 1 (1982).
10. L. A. Silver *et al.*, *ibid.* **104**, 142 (1990).
11. H. Keppler and N. S. Bagdassarov, *Am. Mineral.* **78**, 1324 (1993); M. Nowak and H. Behrens, *Geochim. Cosmochim. Acta* **59**, 3445 (1995).
12. G. Adam and J. H. Gibbs, *J. Chem. Phys.* **43**, 139 (1965).
13. P. Richet and Y. Bottinga, *Rev. Mineral.* **32**, 67 (1995).
14. R. J. Hemley *et al.*, *Nature* **330**, 737 (1987).
15. D. B. Dingwell, C. Romano, K. U. Hess, *Contrib. Mineral. Petrol.* **124**, 19 (1996).
16. M. Takata *et al.*, *J. Am. Ceram. Soc.* **64**, 719 (1981).
17. H. Doweidar, *J. Non-Cryst. Solids* **194**, 155 (1996).
18. J. Schroeder, thesis, Catholic University of America, Washington, DC (1974).
19. H. Eckert *et al.*, *J. Phys. Chem.* **92**, 2055 (1988).
20. We thank A. M. Lejeune for the loan of the samples, G. Boudon and B. Villemant for analyses, and anonymous reviewers for helpful comments. The work was supported by the European Union Training and Mobility of Researchers grant "hydrous melts."

20 March 1998; accepted 4 June 1998

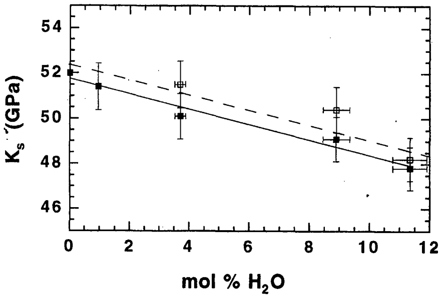

Fig. 3. K_S values of compacted (open squares) and relaxed (solid squares) hydrous andesite glasses. The solid line is a linear fit to the data for the relaxed samples, and the dashed line shows the values that are determined from this fit for the compacted glasses by assuming a value of 4 for K'_0, which is the 1-bar derivative of K_S, and a mean pressure of vitrification of 1.5 kbar.

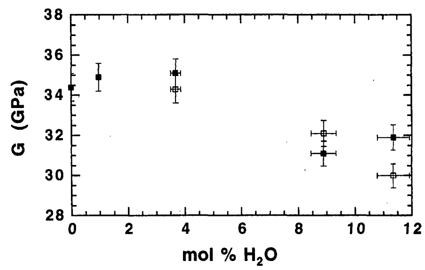

Fig. 4. G values of compacted (open squares) and relaxed (solid squares) hydrous andesite glasses.

Evidence for Large Earthquakes in Metropolitan Los Angeles

Charles M. Rubin,* Scott C. Lindvall, Thomas K. Rockwell

The Sierra Madre fault, along the southern flank of the San Gabriel Mountains in the Los Angeles region, has failed in magnitude 7.2 to 7.6 events at least twice in the past 15,000 years. Restoration of slip on the fault indicated a minimum of about 4.0 meters of slip from the most recent earthquake and suggests a total cumulative slip of about 10.5 meters for the past two prehistoric earthquakes. Large surface displacements and strong ground motions resulting from greater than magnitude 7 earthquakes within the Los Angeles region are not yet considered in most seismic hazard and risk assessments.

The potential for damage from earthquakes along reverse faults in the Los Angeles region has been illustrated by the 1971 San Fernando, 1987 Whittier Narrows, 1991 Sierra Madre, and 1994 Northridge earthquakes (*1*–*3*). These earthquakes have sparked questions regarding the maximum magnitude of earthquakes on reverse faults in the greater Los Angeles region (*4*–*8*) and, in particular, the central Transverse Ranges (*3*, *9*–*14*). Although large events on reverse faults could affect millions of people, most earthquake hazard assessments in southern California have traditionally focused on the San Andreas fault and adjacent strike-slip faults (*15*, *16*). Geodetic studies indicate that the Los Angeles basin from the Jet Propulsion Laboratory to the Palos Verdes Peninsula is shortening by 5 (*10*) to 7.9 mm year^{-1} (*12*), partly along reverse faults. One problem in making an assessment has been that paleoseismic data on these reverse faults are sparse. Here, we present paleoseismic data from the Sierra Madre fault, one of the major reverse faults in

---

C. M. Rubin, Department of Geology, Central Washington University, Ellensburg, WA 98926, USA. S. C. Lindvall, William Lettis and Associates, 27201 Tourney Road, Suite 201-B, Valencia, CA 91355, USA. T. K. Rockwell, Department of Geological Sciences, San Diego State University, San Diego, CA 92182, USA.

*To whom correspondence should be addressed